Yang-Mills two-point functions in linear covariant gauges

A. C. Aguilar,[1] D. Binosi,[2] and J. Papavassiliou[3]

[1] *University of Campinas - UNICAMP,*
Institute of Physics "Gleb Wataghin", 13083-859 Campinas, SP, Brazil

[2] *European Centre for Theoretical Studies in Nuclear Physics*
and Related Areas (ECT) and Fondazione Bruno Kessler,*
Villa Tambosi, Strada delle Tabarelle 286, I-38123 Villazzano (TN) Italy

[3] *Department of Theoretical Physics and IFIC, University of Valencia and CSIC,*
E-46100, Valencia, Spain

Abstract

In this work we use two different but complementary approaches in order to study the ghost propagator of a pure SU(3) Yang-Mills theory quantized in the linear covariant gauges, focusing on its dependence on the gauge-fixing parameter ξ in the deep infrared. In particular, we first solve the Schwinger-Dyson equation that governs the dynamics of the ghost propagator, using a set of simplifying approximations, and under the crucial assumption that the gluon propagators for $\xi > 0$ are infrared finite, as is the case in the Landau gauge ($\xi = 0$). Then we appeal to the Nielsen identities, and express the derivative of the ghost propagator with respect to ξ in terms of certain auxiliary Green's functions, which are subsequently computed under the same assumptions as before. Within both formalisms we find that for $\xi > 0$ the ghost dressing function approaches zero in the deep infrared, in sharp contrast to what happens in the Landau gauge, where it known to saturate at a finite (non-vanishing) value. The Nielsen identities are then extended to the case of the gluon propagator, and the ξ-dependence of the corresponding gluon masses is derived using as input the results obtained in the previous steps. The result turns out to be logarithmically divergent in the deep infrared; the compatibility of this behavior with the basic assumption of a finite gluon propagator is discussed, and a specific Ansatz is put forth, which readily reconciles both features.

PACS numbers: 12.38.Aw, 12.38.Lg, 14.70.Dj

I. INTRODUCTION

The infrared (IR) behavior of Yang-Mills Green's functions in the Landau gauge has been the subject of numerous studies in the past few years, both in the continuum and on the lattice. Particularly important in this challenging quest has been the two-point sector of the theory, where it has been firmly established [1–5] that the gluon propagator saturates in the deep IR, a behavior directly associated with the dynamical generation of a momentum-dependent gluon mass [6–13], and that the ghost propagator remains massless, being accompanied by a dressing function that reaches a finite value at the origin [14, 15][1]. Interestingly enough, these characteristic features persist when implementing the transition from pure Yang-Mills to real world QCD; specifically, the inclusion of a small number of dynamical light quarks induces quantitative but not qualitative changes to the gluon and ghost propagators [20–24].

Given that the Green's functions depend on both the gauge-fixing scheme employed and the choice of the gauge fixing parameter (gfp), it is important to explore their main dynamical features in different gauges, in order to filter out the truly gauge-independent properties of the theory. In particular, it would be interesting to establish the extent of validity and the possible modifications induced to the underlying mechanisms that endow the fundamental degrees of freedom, namely quarks and gluons, with their corresponding dynamical masses. Furthermore, even though physical observables are ostensibly gauge-independent, nonperturbative calculations are subject to truncations, which in turn may distort the delicate conspiracy of terms that produce the required gauge cancellations. It would be therefore a useful exercise to probe explicitly the gauge-(in)dependence of certain special combinations of Green's functions that are extensively used in a variety of phenomenological applications [25–31].

Among the different classes of gauges, the linear covariant (or R_ξ) gauges [32] hold a prominent position. The corresponding gauge-fixing term that must be added to the standard Yang-Mills Lagrangian is given by $\frac{1}{2\xi}(\partial^\mu A^a_\mu)^2$, where ξ represents the gfp; some characteristic values include the aforementioned Landau gauge ($\xi = 0$) and the Feynman gauge ($\xi = 1$). R_ξ gauges have the advantage of manifest Lorentz covariance, and are particularly

[1] For additional studies and alternative approaches, see *e.g.*, [16–19] and references therein.

easy to use in diagrammatic calculations. In addition, by using the novel algorithm proposed in [33], they can be implemented in numerical simulations of lattice regularized Yang-Mills theories even for $\xi \neq 0$ [34].

In the present work we initiate a study of the IR dynamics of the Yang-Mills two-point functions within this latter class of gauges, with the main objective to go beyond the standard Landau gauge paradigm. To that end, we will resort to two distinct but complementary approaches: on the one hand the Schwinger-Dyson equations (SDEs) [35] of the theory, and on the other the so-called Nielsen identities (NIs) [36, 37].

Within the SDE context, we focus exclusively on the integral equation governing the dynamics of the ghost dressing function, $F(q^2)$, which has a much simpler structure than the corresponding equation for the gluon propagator.At the formal level, the SDE in question is written down for general ξ, and after approximating the ghost-gluon vertex by its tree-level value, the solutions are obtained for the range $0 < \xi \leq 1$, thus spanning the values between the Landau and the Feynman gauges.Our main finding is that, contrary to what occurs in the Landau gauge, $F(q^2)$ vanishes as $q^2 \to 0$ for all values of ξ within the aforementioned interval. This drastic change in the infrared behaviour of $F(q^2)$ away from the Landau gauge may be traced back to the massless contributions associated with the ξ-dependent part of the gluon propagator entering into the ghost SDE. Specifically, even if one assumes that the cofactor $\Delta(q^2)$ of the transverse part of the gluon propagator is finite in the deep IR (as happens in the Landau gauge), it is a text-book fact that the longitudinal part (proportional to ξ) receives no quantum corrections, and maintains its tree-level form [see Eq. (2.2)]. This massless contribution, in turn, introduces an infrared divergence into the ghost SDE, which, within the approximations employed, can be counteracted only if the solution for $F(q^2)$ vanishes in the deep IR. In particular, as we will see in detail, $F(q^2)$ vanishes at the very mild rate of $(-c\,\xi \log q^2/\mu^2)^{-1/2}$ (with $c > 0$).

We then turn to the NIs, which express the gauge-dependence of ordinary Green's functions (propagators, vertices, etc.) in terms of special auxiliary functions associated with the extended Becchi-Rouet-Stora-Tyutin (BRST) sector of the theory[2]. In the case of the ghost

[2] The gfp-dependence of Green's functions can be in principle obtained also by using the so-called Landau-Khalatnikov-Fradkin (LKF) transformations [38, 39]. These transformations have been used only in an Abelian context and are in general formulated in position space; therefore, their use for the problem at hand appears to be less direct.

dressing function, the corresponding NI permits us to estimate its first derivative of $F(q^2)$ with respect to ξ, for arbitrary values of ξ; however, for practical purposes we limit our analysis to those ξ that satisfy the condition $\xi \ll 1$. The reason for this choice is that, in this particular limit, the auxiliary functions appearing in the NI may be computed in their one-loop dressed approximation, using as input the gluon and ghost propagators known from the Landau gauge. The emerging expressions, when evaluated in the deep infrared, reproduce rather faithfully the behavior obtained from the ghost SDE; specifically, up to a multiplicative factor, one recovers precisely the derivative of $(-c\,\xi \log q^2/\mu^2)^{-1/2}$ with respect to ξ.

Finally, taking advantage of the NI-based machinery developed here, we go one step further, and study the ξ-dependence of the gluon two-point function, which, in the low momentum region under scrutiny translates directly into a statement on the dynamically generated gluon mass. The relevant auxiliary functions are evaluated using again the approximations and assumptions employed in the previous case. The result reveals that the ξ-derivative of the gluon mass displays an IR logarithmic divergence, which can be traced back to the masslessness of the ghost propagator. As we explain in terms of an explicit example, such a divergent derivative may originate from perfectly IR finite gluon propagators, such as those found in the lattice simulations of [34] for $\xi \ll 1$.

The article is organized as follows. In Sect. II we set up the R_ξ ghost gap equation, discuss the approximations and assumptions employed, and present its numerical solutions, paying particular attention to the deep IR behavior. In Sect. III we address the same problem from the point of view of the NIs. Focusing on the identity satisfied by the ghost dressing function, we evaluate it numerically within the one-loop dressed approximation, which allows for the determination of the leading IR behavior of F. The result turns out to be in excellent qualitative agreement with that found in the previous section. In Sect. III C the NI analysis is extended to the gluon propagator. In particular, a constraint on the IR behavior of the dynamical gluon mass is obtained, and an Ansatz for the possible ξ-dependence of the gluon mass is proposed. Our conclusions are presented in Sect. IV. Finally, the technical details necessary to derive the Yang-Mills NIs are summarized in Appendix A.

II. SCHWINGER-DYSON EQUATION ANALYSIS

In this section we carry out a general analysis of the SDE that governs the ghost propagator, and eventually its dressing function.

A. General considerations and approximations

The ghost gap equation (Fig. 1) can be obtained directly from the one-loop ghost self-energy equation by fully dressing the internal gluon and ghost lines and one of the gluon ghost vertices appearing in it [35]. Dressing the right vertex, the SDE for the ghost propagator in a linear covariant gauge reads (factoring out the trivial color structure δ^{ab})

$$\begin{aligned} D^{-1}(q^2) &= q^2 - i\Pi(q^2) \\ &= q^2 + ig^2 C_A \int_k (k+q)^\mu D(k+q)\Delta_{\mu\nu}(k)\Gamma^\nu(k+q,-k,-q), \end{aligned} \tag{2.1}$$

where $\Pi(q^2)$ represent the ghost self-energy, C_A is the Casimir eigenvalue of the adjoint representation, and the integral measure is defined as $\int_k \equiv \mu^\epsilon/(2\pi)^d \int \mathrm{d}^d k$, with μ the 't Hooft mass and $d = 4-\epsilon$ the dimension of the space-time. $\Delta_{\mu\nu}$ and D denote, respectively, the R_ξ gluon and ghost propagators, defined according to[3]

$$\begin{aligned} &i\Delta_{\mu\nu}(q) = -i\left[P_{\mu\nu}(q)\Delta(q^2) + \xi\frac{q_\mu q_\nu}{q^4}\right]; \qquad P_{\mu\nu}(q) = g_{\mu\nu} - \frac{q_\mu q_\nu}{q^2}, \\ &iD(q^2) = i\frac{F(q^2)}{q^2}, \end{aligned} \tag{2.2}$$

where ξ is the non-negative gfp [32] (see also Appendix A 1), and $F(q^2)$ is the so-called ghost "dressing function". Γ^ν represents the full ghost-gluon vertex, with (all momenta entering)

$$\Gamma^\nu(q_1+q_2,-q_1,-q_2) = \mathcal{A}(q_1+q_2,-q_1,-q_2)q_2^\nu + \mathcal{B}(q_1+q_2,-q_1,-q_2)q_1^\nu, \tag{2.3}$$

where q_1 (q_2) is the gluon (antighost) momentum; at tree-level, $\mathcal{A}^{(0)} = 1$ and $\mathcal{B}^{(0)} = 0$.

Then, using Eqs. (2.2) and (2.3), we may rewrite Eq. (2.1) as

$$\begin{aligned} D^{-1}(q^2) = q^2 &+ ig^2 C_A q^\mu q^\nu \int_k D(k+q)\Delta(k)P_{\mu\nu}(k)\mathcal{A} \\ &+ i\xi g^2 C_A \int_k D(k+q)\left(1+\frac{k\cdot q}{k^2}\right)\left(\mathcal{B}+\frac{k\cdot q}{k^2}\mathcal{A}\right), \end{aligned} \tag{2.4}$$

[3] Our conventions can be found in Appendix A.

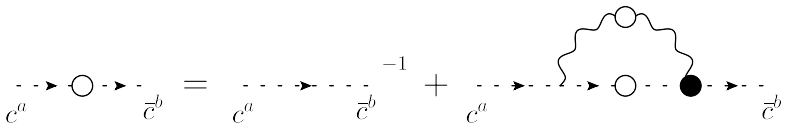

FIG. 1: The ghost gap equation. White (respectively, black) blobs represent connected (respectively, one-particle irreducible) Green's functions.

where the common argument $(k+q, -k, -q)$ of the form factors $\mathcal{A}$ and $\mathcal{B}$ has been suppressed.

Solving this equation in its full generality would require either independent knowledge of the gluon propagator and the form factors of the ghost vertex for general ξ, or to couple (2.4) to the corresponding SDEs describing Δ, $\mathcal{A}$ and $\mathcal{B}$. However, apart from the lattice study of [34], which investigated the gluon propagator for very small values of ξ ($\xi < 10^{-3}$) , there is no direct knowledge of the aforementioned quantities. As for solving the full coupled system of SDEs, unfortunately it constitutes a task that lies beyond our present powers.

Therefore, we will instead study the SDE of Eq. (2.4) within the one-loop dressed approximation, which is obtained by keeping the propagators fully dressed and assigning tree-level values to $\mathcal{A}$ and $\mathcal{B}$. In addition, we will approximate the $\Delta(q^2)$ appearing in the first term on the right-hand side (rhs) of Eq. (2.4) by the Landau gauge propagator $\Delta_{\rm L}(q^2)$. The main underlying assumptions behind this later approximation are that $\Delta(q^2)$ saturates in the IR, assuming the standard form

$$\Delta^{-1}(q^2) = q^2 J(q^2) - m^2(q^2), \tag{2.5}$$

and that the deviation between $\Delta^{-1}(q^2)$ and $\Delta_{\rm L}(q^2)$ in the intermediate momenta region is relatively mild, at least for $0 \leq \xi \leq 1$. Of course, as one approaches the region of larger momenta, the perturbative behavior will eventually set in; at one-loop order, $\Delta^{-1}(q^2)$ renormalized in the momentum-subtraction (MOM) scheme is given by

$$\Delta^{-1}(q^2) \sim q^2 J(q^2) = q^2 \left[1 + \frac{\alpha_s C_A}{8\pi}\left(\frac{13}{3} - \xi\right)\log\frac{q^2}{\mu^2}\right], \tag{2.6}$$

where μ is the renormalization point. For example, for the typical values used in this work, *i.e.*, $\mu = 4.3$ and $\alpha(\mu^2) = 0.22$, the difference between the Landau and Feynman gauge perturbative tails is no more than 7% in the momenta range $2 \div 5$ GeV. In any case, as will become clear in the ensuing analysis, the behavior of $F(q^2)$ in the deep IR is not particularly sensitive to the above considerations; in fact, the complete knowledge of the gluon propagator would only affect the subleading terms.

Thus, the simplified version (2.4) that we will consider is given by

$$D^{-1}(q^2) = q^2 + ig^2 C_A \int_k D(k+q) \left[q^\mu q^\nu \Delta_{\rm L}(k) P_{\mu\nu}(k) + \xi \left(1 + \frac{k\cdot q}{k^2} \right) \frac{k\cdot q}{k^2} \right]. \tag{2.7}$$

This particular integral equation must be properly renormalized, through the introduction of the appropriate renormalization constants for D, $\Delta_{\rm L}$, and ξ. As is well-known, in principle the complete renormalization procedure must be carried out multiplicatively. As a result, in addition to the ghost renormalization constant Z_c that will multiply the tree level term q^2, further constants multiplying the remaining terms on the rhs of Eq. (2.7) must be included; this, in turn, adds an inordinate amount of complexity to the entire problem. Following the standard approximation, we will simply replace $q^2 \to Z_c q^2$, and set all multiplicative constants equal to unity, thus employing subtractive instead of multiplicative renormalization [40, 41]. The actual expression for Z_c is fixed from Eq. (2.7) through the momentum subtraction (MOM) renormalization condition $D_{\rm R}^{-1}(\mu_{\rm R}^2) = \mu_{\rm R}^2$, where $\mu_{\rm R}^2$ is the renormalization point.

As an elementary check, we may recover from Eq. (2.7) the one-loop expression for $F(q^2)$. In particular, setting tree-level values for $D(k+q)$ and $\Delta_{\rm L}(k)$, it is straightforward to show that

$$F^{-1}(q^2) = 1 + \frac{ig^2 C_A}{4} \left[(3-\xi) \int_k \frac{1}{k^2 (k+q)^2} + 2(1-\xi) \int_k \frac{k\cdot q}{k^4 (k+q)^2} \right]. \tag{2.8}$$

Using standard integration formulas, setting $q_{\rm E}^2 = -q^2$, and renormalizing in the aforementioned scheme, one obtains for the renormalized ghost dressing function

$$F_{\rm R}^{-1}(q_{\rm E}^2) = 1 + \frac{\alpha_s C_A}{16\pi} (3-\xi) \log(q_{\rm E}^2/\mu^2), \tag{2.9}$$

where we have defined $\alpha_s = g^2/4\pi$.

B. Numerical analysis

After a set of basic algebraic manipulations, together with the shift $k+q \to k$, we may cast Eq. (2.7) in the form

$$D^{-1}(q^2) = q^2 + ig^2 C_A \int_k D(k) \left\{ \frac{q^2 k^2 - (k\cdot q)^2}{(k+q)^2} \Delta_{\rm L}(k+q) + \frac{\xi}{4} \left[\frac{(k^2-q^2)^2}{(k+q)^4} - 1 \right] \right\}. \tag{2.10}$$

This last form of the ghost SDE is more convenient for the numerical analysis that follows, because it allows us to carry out exactly the angular integration in the term proportional

to ξ, while in the first term the angular dependence has been passed from the unknown function $D(k+q)$ to the function $\Delta_{\rm L}(k)$, which is known from the lattice.

In order to solve this equation, we first pass to Euclidean space using the standard substitution rules

$$\mathrm{d}^4k \to i\mathrm{d}^4k_{\rm E};\quad (q^2,k^2,k\cdot q)\to(-q^2_{\rm E},-k^2_{\rm E},-k_{\rm E}\cdot q_{\rm E});\quad \Delta(q^2),D(q^2)\to-\Delta_{\rm E}(q^2_{\rm E}),-D_{\rm E}(q^2_{\rm E}), \tag{2.11}$$

and suppress throughout the subscript "E" in what follows. Next, we introduce spherical coordinates (in $d=4$), through the relations

$$\begin{aligned} &x=q^2;\qquad y=k^2;\qquad z=(k+q)^2=x+y+2\sqrt{xy}\cos\theta;\\ &\int_{k_{\rm E}}=\frac{1}{(2\pi)^3}\int_0^\pi \mathrm{d}\theta\,\sin^2\theta\int_0^\infty \mathrm{d}y\,y, \end{aligned} \tag{2.12}$$

use the result

$$\int_0^\pi \mathrm{d}\theta\,\frac{\sin^2\theta}{z^2}=\frac{\pi}{2}\left[\frac{1}{x(x-y)}\Theta(x-y)+\frac{1}{y(y-x)}\Theta(y-x)\right], \tag{2.13}$$

where $\Theta(x)$ is the Heaviside function, and factor out a q^2 from both sides of Eq. (2.10). Thus, we obtain the final equation for the (subtractively renormalized) ghost dressing function $F(x)$,

$$\begin{aligned} F^{-1}(x)=Z_c-\frac{\alpha_s C_A}{2\pi^2}\int_0^\infty \mathrm{d}y\,y\,F(y)\int_0^\pi \mathrm{d}\theta\,\frac{\sin^4\theta}{z}\Delta_{\rm L}(z)\\ +\xi\frac{\alpha_s C_A}{16\pi}\left[\frac{1}{x^2}\int_0^x \mathrm{d}y\,yF(y)+\int_x^\infty \mathrm{d}y\,\frac{F(y)}{y}\right], \end{aligned} \tag{2.14}$$

Before proceeding to the full numerical treatment of this integral equation, it would be useful to identify some of its main IR features by means of a more direct method. In particular, if we assume that the $F(x)$ reaches a finite value in the IR ($x\to 0$), inspection of Eq. (2.14) reveals that the dominant term in that momentum region is the last one. Indeed, the first term corresponds *qualitatively* to the Landau gauge case: if the gluon propagator ($\Delta_{\rm L}$) saturates in the IR, this term is finite. The second term is also finite in the IR, as the simple change of variable $y=tx$ immediately demonstrates. Therefore, keeping only the dominant IR contribution on the rhs of Eq. (2.14) we obtain

$$F^{-1}(x)\underset{x\to 0}{\sim}\xi\frac{\alpha_s C_A}{16\pi}\int_x^\infty \mathrm{d}y\,\frac{F(y)}{y}. \tag{2.15}$$

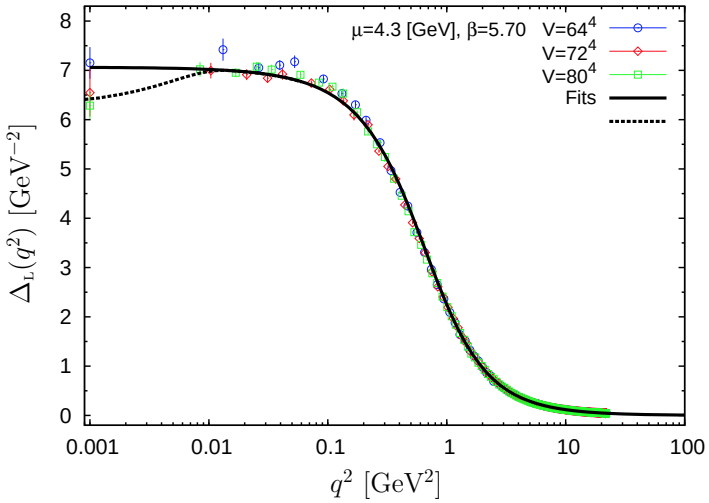

FIG. 2: (color online). The lattice SU(3) gluon propagator evaluated in the Landau gauge [4] and the corresponding fit used in our calculation [27]. The dashed curve shows a fit featuring an IR maximum which is due to the presence of (divergent) contributions to the gluon (inverse) dressing function [42]. All functions are renormalized at $\mu = 4.3$ GeV.

This integral equation can be converted into a differential equation, by differentiating both sides with respect to x; we then obtain

$$F'(x) \underset{x\to 0}{\sim} \xi c \frac{F^3(x)}{x}; \qquad c = \frac{\alpha_s C_A}{16\pi}, \tag{2.16}$$

which is solved by

$$F(x) \underset{x\to 0}{\sim} \pm \frac{1}{\sqrt{a - 2\xi c \log(x/\mu^2)}}, \tag{2.17}$$

with a a (possibly ξ dependent) constant, and μ a suitable renormalization scale; the physical solution corresponds to the positive sign. Notice that the IR solution given in Eq. (2.17) requires the aforementioned non-negativity condition $\xi \geq 0$, since otherwise F would become complex; in particular, from now on, we will restrict our attention to $\xi \in [0, 1]$.

Eq. (2.17) predicts an important qualitative modification in the IR behavior of the ghost dressing functions, compared to what is known from the Landau gauge studies. Specifically, whereas in the Landau gauge $F_{\rm L}(0)$ =const, whenever $\xi > 0$ one finds that F is driven to zero at the origin, namely $F(0) = 0$.

We next focus on the complete numerical evaluation of Eq. (2.14). To this end, we will use as input for $\Delta_{\rm L}$ the fit to the available SU(3) lattice data [4] introduced in [27] (see Fig. 2). The value of the renormalization point within the MOM scheme is $\mu = 4.3$ GeV.

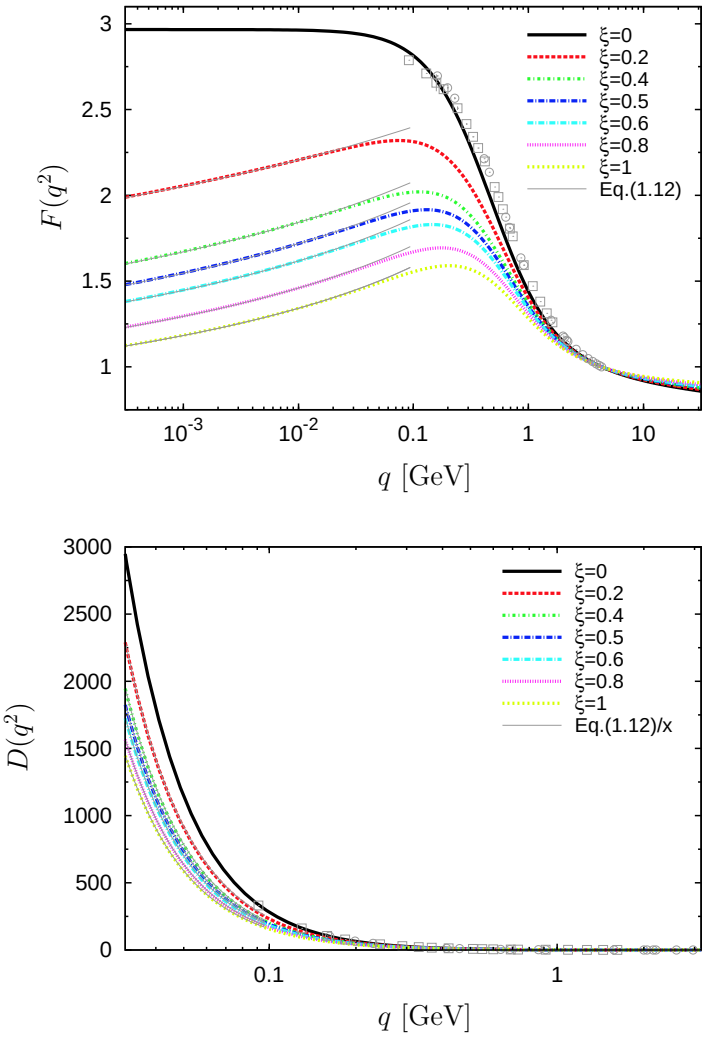

FIG. 3: (color online). Solution of the SDE (2.14) (upper panel) and the associated ghost propagator (lower panel) for various values of the gauge fixing parameter ξ. In the IR the solution obtained is perfectly described by Eq. (2.17) after fitting for determining the value of the arbitrary constant a. For comparison we plot also the Landau gauge lattice data of [4].

Notice that in Fig. 2 we show also a fit displaying an IR maximum that must appear due to the presence of divergent terms contributing to the gluon (inverse) dressing function [42] (see also Sect. III B); however, the results finally obtained from the solution of the SDE are completely insensitive to the implementation of this particular feature in the gluon propagator.

The solutions obtained for $\alpha_s = 0.29$ and gfp values ranging from 0 to 1 are shown in the left panel of Fig. 3. The value of α_s is chosen so that in the Landau gauge $\xi = 0$

one reproduces the lattice data of [4] (see the black continuous curve in Fig. 3); the 30% deviation from the expected value of $\alpha_s = 0.22$ (at $\mu = 4.3$ GeV) is due to the use of the tree-level ghost-vertex, as demonstrated in [43].

One immediately observes the drastic change in the IR behavior of the ghost dressing function: at $\xi = 0$ $F_{\rm L}(0)$ is finite, whereas when $\xi \neq 0$ $F(0)$ vanishes. The IR behavior is precisely the one described by the IR solution (2.17), where

$$a = a(\xi) = 0.12(1 + \xi); \qquad c = 0.035. \tag{2.18}$$

Evidently, the rate at which $F(q^2)$ approaches zero is very slow, and begins to set on at the rather low scale of about 100 MeV (upper panel of Fig. 3). However, the first appreciable deviations from the $F_{\rm L}(q^2)$ obtained in the Landau gauge manifest themselves at the higher scale of about 300 MeV, where the $F(q^2)$ displays a characteristic maximum. This particular feature, in turn, may serve as a guiding signal in future lattice simulations away from the Landau gauge.

The overall effect of $F(q^2)$ on the full ghost propagator $D(q^2)$ is shown in the right panel of Fig. 3. In particular, one observes that the rate of divergence of the ghost propagator at the origin becomes slightly softer compared to that of the Landau gauge.

Let us conclude this section by determining for later convenience the IR behavior of the derivative with respect to ξ of the ghost dressing evaluated at $\xi = 0$; one finds

$$\partial_\xi F(x)|_{\xi=0} \underset{x\to 0}{\sim} c_{\rm SDE} \log\frac{x}{\mu^2} \times F_{\rm L}(0); \qquad\qquad c_{\rm SDE} = \frac{\alpha_s C_A}{16\pi}\frac{1}{a(0)}, \tag{2.19}$$

where we have used the fact that $F_{\rm L}(0) = 1/\sqrt{a(0)}$. Clearly, this quantity displays an IR logarithmic divergence; substituting the numerical values of the constants involved one obtains $c_{\rm SDE} = 0.15$.

III. NIELSEN IDENTITIES

In this section we take a different but complementary look at the problem, by resorting to a set of identities originally introduced by Nielsen [36, 37]; for all technical details the reader is referred to Appendix A, where the general derivation is summarized.

A. Ghost propagator

Consider the ghost two-point sector of the theory. The corresponding NI is readily obtained by differentiating the functional identity (A20) with respect to one antighost and one ghost field; setting afterwards all fields and sources to zero, one obtains the relation

$$\partial_\xi \Gamma_{c^a \bar{c}^b}(q^2) = i\Gamma_{\bar{c}^b \chi A^d_\mu}(q,0,-q)\Gamma_{c^a A^{*\mu}_d}(q) - i\Gamma_{c^a \chi c^*_d}(q,0,-q)\Gamma_{c^d \bar{c}^b}(q^2), \tag{3.1}$$

where

$$\Gamma_{c^a \bar{c}^b}(q^2) = -i\delta^{ab} q^2 F^{-1}(q^2); \qquad \Gamma_{c\bar{c}}(q^2) = -\Pi(q^2). \tag{3.2}$$

In Eq. (3.1) ϕ^* denotes the antifield associated to the field ϕ. In addition, χ represents the static (*i.e.*, momentum independent) source associated to the gfp ξ; therefore, and despite their appearance, all functions in the identity above are two-point functions.

Eq. (3.1) can be further simplified by noticing that the so-called ghost (or Faddeev-Popov) equation (A17) yields

$$\Gamma_{c^a A^{*b}_\mu}(q) = i\delta^{ab}\frac{q_\mu}{q^2}\Gamma_{c^a \bar{c}^b}(q^2), \tag{3.3}$$

a result which allows to trade the function Γ_{cA^*} in (3.1) for a ghost two-point function $\Gamma_{c\bar{c}}$. Then, factoring out the trivial color structure δ^{ab}, one is left with the identity

$$\partial_\xi \Gamma_{c\bar{c}}(q^2) = -\left[\frac{q^\mu}{q^2}\Gamma_{\bar{c}\chi A_\mu}(q,0,-q) + i\Gamma_{c\chi c^*}(q,0,-q)\right]\Gamma_{c\bar{c}}(q^2). \tag{3.4}$$

In order to appreciate with a concrete example how the NIs work, let us consider the explicit realization of Eq. (3.4) at the one-loop level. The left-hand side (lhs) of Eq. (3.4) can be immediately deduced from Eq. (2.8), yielding

$$\partial_\xi \Gamma^{(1)}_{c\bar{c}}(q^2) = -\frac{g^2 C_A}{4} q^2 \left[\int_k \frac{1}{k^2(k+q)^2} + 2\int_k \frac{k\cdot q}{k^4(k+q)^2}\right]. \tag{3.5}$$

Turning to the rhs of (3.4), the diagrams contributing to the auxiliary functions $\Gamma_{\bar{c}\chi A_\mu}$ and $\Gamma_{c\chi c^*}$ at one-loop level are shown in Fig. 4. Using the Feynman rules reported in Appendix A and Ref. [44], one has the results

$$\begin{aligned} i\Gamma^{(1)}_{\bar{c}\chi A_\mu}(q,0,-q) &= \frac{g^2 C_A}{2}\left[q_\sigma \int_k \frac{1}{k^4} P^\sigma_\mu(k+q) - \int_k \frac{k\cdot q}{k^4(k+q)^2}(k+q)_\mu\right], \\ i\Gamma^{(1)}_{c\chi c^*}(q,0,-q) &= i\frac{g^2 C_A}{2}\int_k \frac{k^2 + k\cdot q}{k^4(k+q)^2}. \end{aligned} \tag{3.6}$$

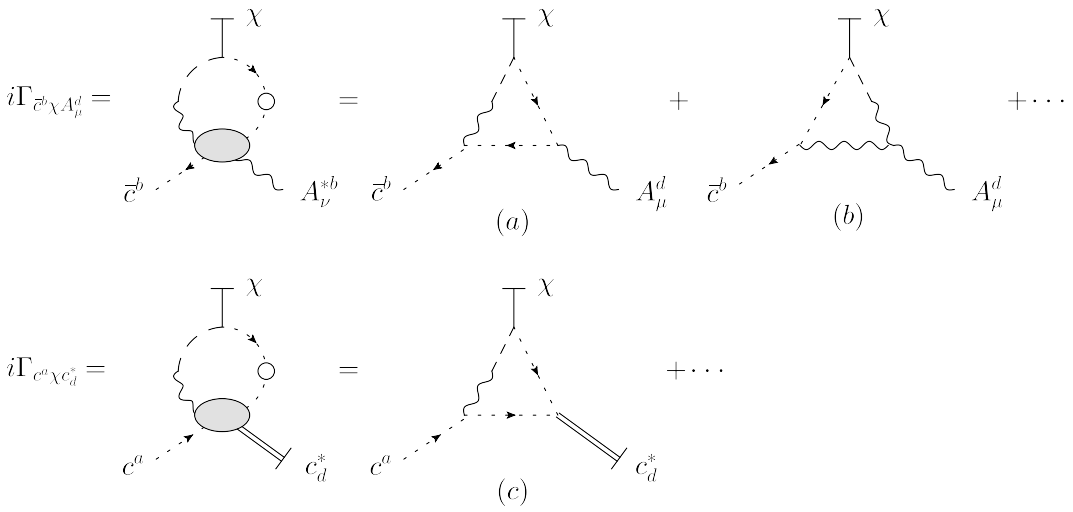

FIG. 4: One-loop diagrams contributing to the auxiliary functions $\Gamma_{\bar{c}\chi A_\mu}$ and $\Gamma_{c\chi c^*}$ appearing in the ghost two-point Nielsen identity (3.1). Notice the presence of the mixed propagator Δ_{bA}.

Notice that the contribution proportional to ξ that could be in principle generated from diagram (b) of Fig. 4 vanishes as a result of the Slavnov-Taylor identity $q_1^\mu q_2^\nu q_3^\rho \Gamma_{\mu\nu\rho}(q_1,q_2,q_3)=0$. Thus one finally has

$$\left[\frac{q^\mu}{q^2}\Gamma^{(1)}_{\bar{c}\chi A_\mu}(q,0,-q)+i\Gamma^{(1)}_{c\chi c^*}(q,0,-q)\right]\Gamma^{(0)}_{c\bar{c}}(q^2)=\frac{g^2C_A}{4}q^2\left[\int_k\frac{1}{k^2(k+q)^2}+2\int_k\frac{k\cdot q}{k^4(k+q)^2}\right], \tag{3.7}$$

which, in view of Eq. (3.5), confirms the validity of Eq. (3.4) at one-loop.

B. Small ξ limit and the one-loop dressed approximation

Consider now the limit $\xi \ll 1$; in this case, one can set $\xi=0$ on both sides of Eq. (3.4), and use Eq. (3.2) to obtain

$$\partial_\xi F(q^2)\big|_{\xi=0} = -\left[\frac{q^\mu}{q^2}\Gamma^{\rm L}_{\bar{c}\chi A_\mu}(q,0,-q)+i\Gamma^{\rm L}_{c\chi c^*}(q,0,-q)\right]F_{\rm L}(q^2), \tag{3.8}$$

where the auxiliary ghost functions appearing on the rhs are now evaluated in the Landau gauge (see also the discussion at the end of Appendix A 1). This last equation can be used to deduce the IR behavior of $F(q^2,\xi)$ from the knowledge of the basic Green's functions in the Landau gauge. In particular, it allows us to compare the result obtained from the direct evaluation of the rhs of Eq. (3.8) in the limit $q^2\to 0$ with the corresponding expression derived in Eq. (2.19) in the SDE context. To this end, we will study the auxiliary functions

$\Gamma^{\rm L}_{\bar{c}\chi A_\mu}$ and $\Gamma^{\rm L}_{c\chi c^*}$ in the one-loop dressed approximation, in which the diagrams contributing to each function are obtained from those shown in Fig. 4 by fully dressing the propagators, while keeping all vertices at their tree-level values[4]. The simple inspection of the diagrams given in Fig. 4 suggests that, indeed, a logarithmic behavior similar to that of Eq. (3.8) is expected to make its appearance. This is because diagrams (a) and (c) may be essentially regarded as closed ghost loops, which, due to the nonperturbative masslessness of the ghost propagators entering in them, are known to diverge logarithmically in the IR [42, 45].

Let us then evaluate explicitly the one-loop dressed expressions of $\Gamma^{\rm L}_{\bar{c}\chi A_\mu}$ and $\Gamma^{\rm L}_{c\chi c^*}$; one has the following results

$$\begin{aligned}\frac{q^\mu}{q^2}\Gamma^{\rm L}_{\bar{c}\chi A_\mu}(q,0,-q) &\underset{\rm 1ldr}{=} i\frac{g^2C_A}{2}\left[\int_k \frac{(k\cdot q)(k\cdot q+q^2)}{q^2k^4(k+q)^2}F_{\rm L}(k)F_{\rm L}(k+q)\right.\\ &\qquad\left.-\int_k\frac{k^2q^2-(k\cdot q)^2}{q^2k^4}F_{\rm L}(k)\Delta_{\rm L}(k+q)\right],\\ i\Gamma^{\rm L}_{\bar{c}\chi c^*}(q,0,-q) &\underset{\rm 1ldr}{=} i\frac{g^2C_A}{2}\int_k\frac{k^2+k\cdot q}{k^4(k+q)^2}F_{\rm L}(k)F_{\rm L}(k+q).\end{aligned}\tag{3.9}$$

The terms proportional to the product of two ghost dressing functions $F_{\rm L}$ in both functions are those corresponding to the aforementioned ghost-loops; therefore, in the deep IR both functions display a logarithmic divergence, so that, in turn, one has

$$\partial_\xi F(q^2)\big|_{\xi=0}\underset{q^2\to 0}{\sim} c_{\rm NI}\log\frac{q^2}{\mu^2}\times F_{\rm L}(0),\tag{3.10}$$

where $c_{\rm NI}$ a suitable constant and μ the renormalization scale chosen. Notice that this is exactly the kind of behavior found in Eq. (2.19) from the SDE analysis.

The qualitative agreement between Eq. (2.19) and Eq. (3.10) motivates a further quantitative study, focusing on the actual value of the coefficient c obtained within the two methods (SDE vs NI). To accomplish this, we evaluate numerically the one-loop dressed

[4] Note that the b-equation (A14) implies that every Green's function which involves the Nakanishy-Lautrup multiplier b remains fixed at its tree-level value: therefore in the b-sector the one-loop dressed approximation is exact.

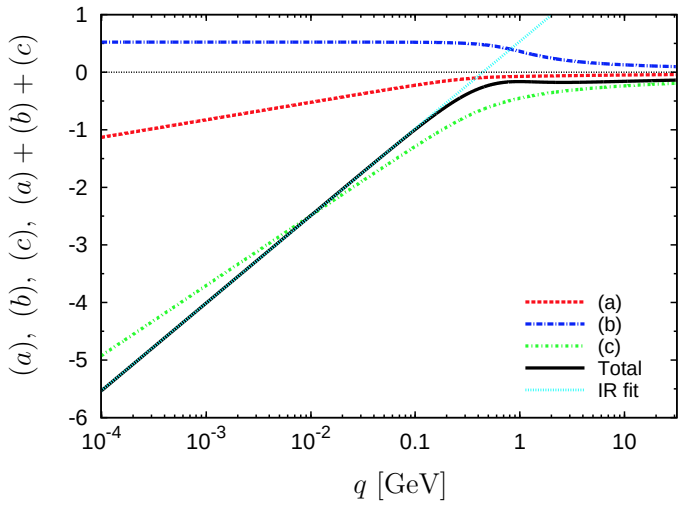

FIG. 5: (color online). Contributions of the one-loop dressed auxiliary functions to the ghost two-point function Nielsen identity. The IR region is perfectly described by the predicted $c_{\rm NI}\log q^2/\mu^2$ behavior yielding $c_{\rm NI}=0.33$.

contributions (3.9), which are given by (Euclidean space)

$$\begin{aligned}\frac{q^\mu}{q^2}\Gamma^{\rm L}_{\bar{c}\chi A}(q,0,-q) &\underset{\rm 1ldr}{=} \frac{g^2C_A}{2(2\pi)^3}\int_0^\pi {\rm d}\theta\,\sin^2\theta\cos\theta\int_0^\infty {\rm d}y\,\left(\cos\theta+\sqrt{\frac{x}{y}}\right)\frac{1}{z}F_{\rm L}(y)F_{\rm L}(z)\\ &+\frac{g^2C_A}{3(2\pi)^3}\int_0^\pi {\rm d}\theta\,\sin^4\theta\int_0^\infty {\rm d}y\,F_{\rm L}(y)\Delta_{\rm L}(z)=(a)+(b),\\ i\Gamma^{\rm L}_{\bar{c}\chi c^*}(q,0,-q) &\underset{\rm 1ldr}{=} -\frac{g^2C_A}{2(2\pi)^3}\int_0^\pi {\rm d}\theta\,\sin^2\theta\int_0^\infty {\rm d}y\,\left(1+\sqrt{\frac{x}{y}}\cos\theta\right)\frac{1}{z}F_{\rm L}(y)F_{\rm L}(z)=(c),\end{aligned}\tag{3.11}$$

where (a), (b) and (c) denote the contributions of the diagrams appearing in Fig. 4. At this point all integrals can be evaluated provided that we supply as input the Landau gauge gluon propagator $\Delta_{\rm L}$ and the ghost dressing function $F_{\rm L}$ (see Fig. 2 and Fig. 3, respectively).

The results obtained for the three individual terms (a), (b) and (c) of Eq. (3.11), as well as their sum, are shown on the left-panel of Fig. 5. One sees that terms (a) and (c) show the claimed logarithmic divergence, while in the case of (b) the gluon mass acts as an IR regulator, making the integral convergent. Adding the three contributions together one obtains the black continuous curve of Fig. 5, yielding the IR behavior (3.10) with $c_{\rm NI}=0.33$; this value should be compared to the value $c_{\rm SDE}=0.15$ obtained from the SDE analysis. Given that the two values are derived from two *a priori* completely distinct methods, we find the proximity between the two values rather encouraging.

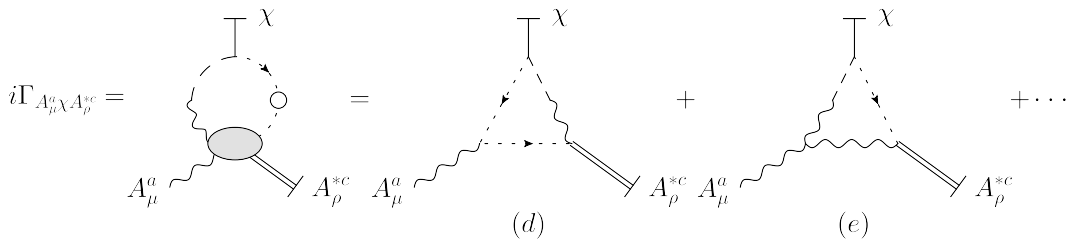

FIG. 6: One-loop diagrams contributing to the auxiliary function $\Gamma_{A_\mu \chi A^*_\nu}$ appearing in the gluon two-point Nielsen identity (3.12).

C. Gluon propagator

The NI formalism may be extended in a straightforward way to the case of the gluon propagator. Specifically, the corresponding NI for the gluon two-point function Γ_{AA} can be derived by differentiating Eq. (A20) with respect to two gluon fields, and setting afterwards all fields to zero. In particular, one obtains the equation

$$\partial_\xi \Gamma_{A^a_\mu A^b_\nu}(q) = -i\Gamma_{A^a_\mu \chi A^{*\rho}_c}(q,0,-q)\Gamma_{A^c_\rho A^b_\nu}(q) - i\Gamma_{A^b_\nu \chi A^{*\rho}_c}(q,0,-q)\Gamma_{A^c_\rho A^a_\mu}(q). \tag{3.12}$$

Given that Γ_{AA} is transverse to all orders, with its tree-level value given by $\Gamma^{(0)}_{A^a_\mu A^b_\nu}(q) = iq^2\delta^{ab}P_{\mu\nu}(q)$ (see Appendix A), this identity can be further simplified to read

$$\partial_\xi \Gamma_{AA}(q^2) = -2i\Gamma_{A\chi A^*}(q,0,-q)\Gamma_{AA}(q^2), \tag{3.13}$$

where the color structure has been factored out, and we have defined

$$\Gamma_{A\chi A^*}(q,0,-q) = \frac{1}{d-1}P^{\mu\nu}(q)\Gamma_{A_\mu \chi A^*_\nu}(q,0,-q). \tag{3.14}$$

One can appreciate how the above identity works by evaluating it at lowest order in perturbation theory. The diagrams contributing to the function $\Gamma_{A\chi A^*}$ at the one-loop level are shown in Fig. 6; then the rhs of Eq. (3.13) reads

$$\begin{aligned} -2i\Gamma^{(1)}_{A_\mu \chi A^*_\rho}(q,0,-q)\Gamma^{(0)}_{A^\rho A_\nu}(q) = g^2 C_A q^2 P^\rho_\nu(q) \left\{ \int_k \frac{(k^2-q^2)}{k^2(k+q)^2} P_{\mu\rho}(k) - \int_k \frac{(k+q)_\mu k_\rho}{k^4(k+q)^2} \right. \\ \left. +(1-\xi)q^2 P^\sigma_\mu(q) \int_k \frac{k_\rho k_\sigma}{k^4(k+q)^4} \right\}. \end{aligned} \tag{3.15}$$

To complete the comparison, note that $\Pi^{(1)}_{\mu\nu}(q)$ has been evaluated in [46] [see Eq. (2.56)]; its derivative with respect to ξ coincides with the result (3.15), once we take into account that $\Pi_{\mu\nu}(q) = -\Gamma_{A_\mu A_\nu}(q)$.

Next, we consider the $\xi \ll 1$ limit of Eq. (3.13), obtaining

$$\partial_\xi \Delta^{-1}(q^2)\big|_{\xi=0} = -2i\Gamma^{\rm L}_{A\chi A^*}(q,0,-q)\Delta^{-1}_{\rm L}(q^2); \qquad \Gamma_{AA}(q^2) = i\Delta^{-1}(q^2). \tag{3.16}$$

The rhs of this equation can then be evaluated within the one-loop dressed approximation, yielding the expression

$$\begin{aligned} -2i\Gamma^{\rm L}_{A\chi A^*}(q,0,-q) \underset{\rm 1ldr}{=} & -i\frac{g^2 C_A}{d-1}\left\{\int_k \frac{k^2q^2-(k\cdot q)^2}{q^2k^4(k+q)^2}F_{\rm L}(k)F_{\rm L}(k+q)\right. \\ & \left. + \int_k \frac{k^2-q^2}{(k+q)^4}\left[d-2+\frac{(k\cdot q)^2}{k^2q^2}\right]\Delta_{\rm L}(k)F_{\rm L}(k+q)\right\}. \end{aligned} \tag{3.17}$$

One notices again the presence of a massless ghost loop, which implies in turn the divergent IR behavior

$$\partial_\xi \Delta^{-1}(q^2)\big|_{\xi=0} \underset{q^2\to 0}{\sim} \partial_\xi m^2(q^2)\big|_{\xi=0} \underset{q^2\to 0}{\sim} c_{\rm NI}\log\frac{q^2}{\mu^2}\times m^2_{\rm L}(0), \tag{3.18}$$

where the first expression on the rhs originates from the fact that when $q^2 \to 0$, $\Delta^{-1}(q^2) \to m^2(q^2)$ [see Eq. (2.5)], and $m^2_{\rm L}(q^2)$ denotes the dynamical gluon mass in the Landau gauge [11–13].

The appearance of this particular behavior may be indeed confirmed numerically. Specifically, after passing to the Euclidean metric and introducing spherical coordinates, one obtains

$$\begin{aligned} -2i\Gamma^{\rm L}_{A\chi A^*}(q,0,-q) \underset{\rm 1ldr}{=} & -\frac{g^2C_A}{3(2\pi)^3}\int_0^\pi {\rm d}\theta \sin^4\theta \int_0^\infty {\rm d}y\, \frac{1}{z_1}F_{\rm L}(y)F_{\rm L}(z_1) \\ & + \frac{g^2C_A}{3(2\pi)^3}\int_0^\pi {\rm d}\theta\,(3-\sin^2\theta)\sin^2\theta\int_0^\infty {\rm d}y\,\frac{y(y-x)}{z_1^2}\Delta_{\rm L}(y)F_{\rm L}(z_1) \\ & = (d)+(e), \end{aligned} \tag{3.19}$$

which can be evaluated using the Landau gauge propagator and ghost dressing function introduced before. The results are shown in Fig. 7; one observes a logarithmic IR divergence in diagram (d), while the IR finiteness of diagram (e) is due to the presence of the dynamical gluon mass. When summing everything together the IR behavior is indeed the one described by Eq. (3.10), with $c_{\rm NI} = 0.13$.

Finally, it is rather interesting to consider how the IR divergence found in (3.18) might be reconciled with the underlying assumption of an IR finite gluon propagator. Given that, at present, the dynamical equation that describes the gluon mass has only been derived in the

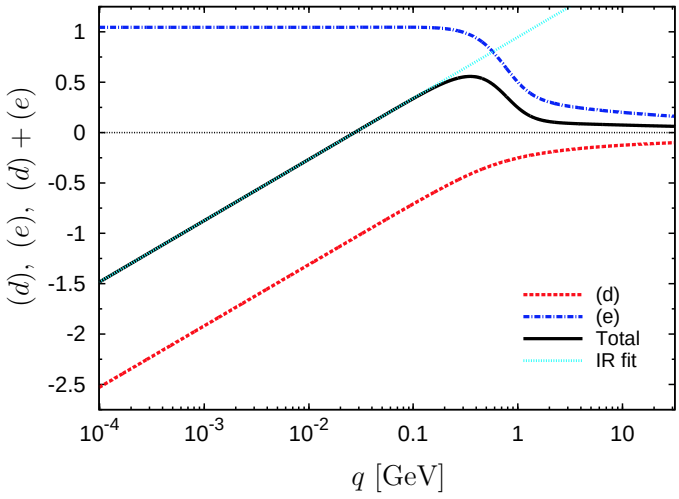

FIG. 7: (color online). Contributions of the one-loop dressed auxiliary functions to the gluon two-point function Nielsen identity. Also in the gluon case the IR region is perfectly described by the predicted $b \log q^2/\mu^2$ behavior, now with $c_{\rm NI} = 0.13$.

Landau gauge[5], one may only proceed by postulating an Ansatz for $m^2(q^2)$ that would satisfy (3.18), and study its consequences at the level of the corresponding gluon propagators.

One such possibility is given by the following Ansatz for the ξ-dependent mass function[6]

$$m^2(q^2) = \left[a(\xi) + c(\xi)\left(\frac{q^2}{\mu^2}\right)^{\xi} \log\frac{q^2}{\mu^2}\right] m^2_{\rm L}(q^2), \tag{3.20}$$

with

$$a(\xi) = a_0 + a_1\xi + \cdots\,; \qquad c(\xi) = c_1\xi + \cdots\,. \tag{3.21}$$

Notice that the (resummed) behavior $\sim (q^2/\mu^2)^{\xi}$ has been also observed when studying the gfp-dependence of fermion propagators through LKF transformations [40, 51].

[5] For related studies in the Coulomb gauge, see [47–50]

[6] A simpler Ansatz would have been

$$m^2(q^2) = \left[a(\xi) + c(\xi)\left(\frac{q^2}{\mu^2}\right)^{\xi}\right] m^2_{\rm L}(q^2),$$

with

$$a(\xi) = 1 - c_0 - a_1\xi + \cdots\,; \qquad c(\xi) = c_0 + \cdots$$

and $c_0 \equiv c_{\rm NI} \approx 0.13$. In this case, however, the limits $\xi \to 0$ and $q^2 \to 0$ do not commute, contrary to what happens with the Ansatz (3.20).

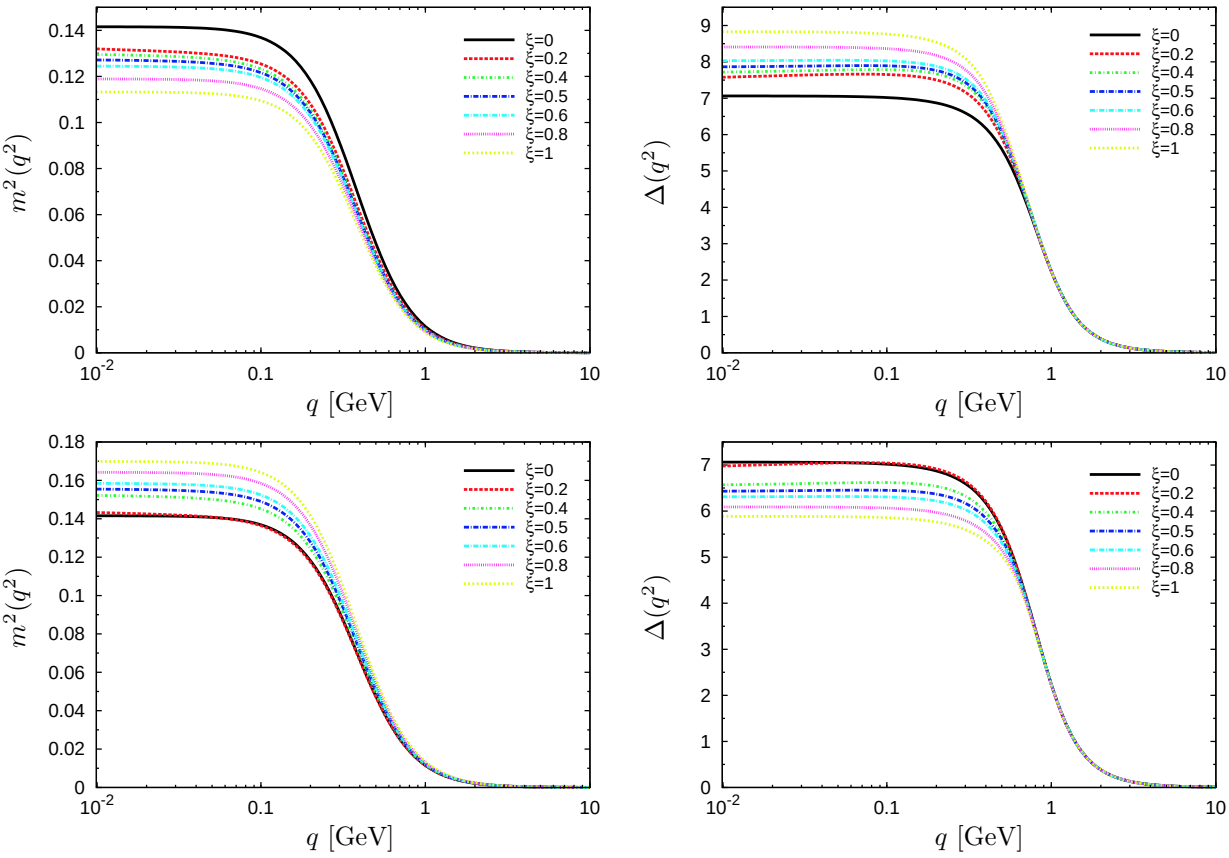

FIG. 8: (color online). ξ-dependence of the gluon mass (left panels) and gluon propagator (right panels) as predicted by the Ansatz (3.20) for $a_1 = -0.2$ (upper panels) and $a_1 = 0.2$ (lower panels).

Evidently, choosing $a_0 = 1$ and $c_1 \equiv c_{\rm NI} = 0.13$ ensures that

$$
\begin{aligned}
m^2(q^2) &\underset{q^2\to 0}{\sim} (1 + a_1\xi) m^2_{\rm L}(0), \\
\partial_\xi m^2(q^2)\big|_{\xi=0} &\underset{q^2\to 0}{\sim} c \log\frac{q^2}{\mu^2} \times m^2_{\rm L}(0),
\end{aligned}
\tag{3.22}
$$

in agreement with (3.18); in addition, small values of a_1 would make the R_ξ and Landau-gauge propagators and dynamical masses to be rather close to each other, justifying in retrospect our replacing Δ by $\Delta_{\rm L}$ when solving the ghost SDE.

Evidently, within this approach, the sign of the coefficient a_1 remains undetermined. This sign, in turn, controls the leading behavior of the gfp-dependence of the gluon mass (and correspondingly of the propagator) in the deep IR: a positive a_1 implies an increasing (decreasing) mass (propagator), while for a_1 negative the behavior would be reversed. This is shown in Fig. 8, where the left panels depict the ξ-dependence of the gluon dynamical

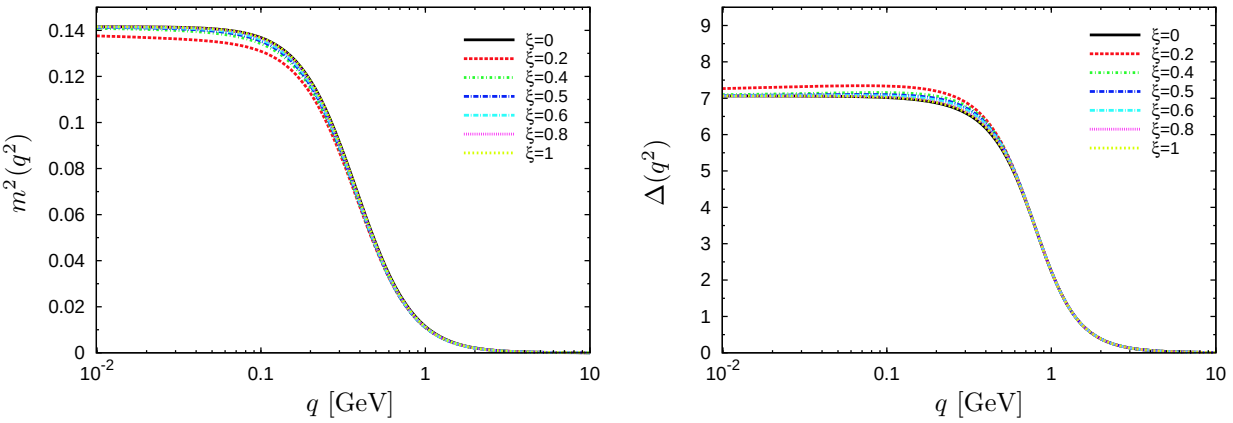

FIG. 9: (color online). ξ-dependence of the gluon mass (left) and gluon propagator (right) as predicted by the Ansatz (3.20) for $a_1 = 0$.

mass (3.20) for the two values $a_1 = 0.2$ (upper-left) and $a_1 = -0.2$ (lower left), while the corresponding gluon propagators, obtained from the relation $\Delta^{-1}(q^2) = q^2 J_{\rm L}(q^2) + m^2(q^2)$, are shown on the right panels of the same figure.

Notice that the case $a_1 = 0$ would be particularly interesting, as it would imply that, at leading order in ξ, the R_ξ gluon mass and propagator coincide in the IR with the corresponding quantities computed in the Landau gauge. In addition, as can be appreciated from Fig. 9, the ξ-dependence over the entire range of momenta would be minimal.

IV. CONCLUSIONS

In the present work we have analyzed the nonperturbative behavior of Yang-Mills Green's functions quantized in a linear covariant gauge, paying particular attention to its dependence on the parameter ξ characterizing this class of gauges. We have first focussed on the ghost two-point function and shown that, within a well-defined set of approximations, the solutions of the corresponding SDE for $\xi > 0$ are such that the dressing function $F(q^2)$ vanishes as $q^2 \to 0$; this is in sharp contrast to the Landau gauge case ($\xi = 0$) where $F(q^2)$ is known to saturate in the low momentum region. The particular IR behavior found for $F(q^2)$ turned out to be in notable agreement with that obtained from the Nielsen identity satisfied by this function, within the one-loop dressed approximation and for $\xi \ll 1$. The NI analysis has been then extended to the gluon two-point function, and shown to predict the same kind

of logarithmic divergence for the derivative with respect to ξ of the dynamical gluon mass, $\partial_\xi m^2(q^2)|_{\xi=0} \sim c \log q^2/\mu^2 \times m_{\rm L}^2(0)$. A particular example of a $m^2(q^2)$ that reconciles this behavior with the assumed saturation of the gluon propagator away from the Landau gauge was given, and its main features were studied numerically.

Undoubtedly, lattice simulations would be crucial for verifying or amending the findings of this preliminary SDE study. As already mentioned, exploratory simulations in the linear gauges have already been carried out for the gluon propagator [34]; it would be interesting to extend them to larger values of ξ, in order to determine whether the observed IR saturation persists. Furthermore, the IR suppression of the ghost dressing function predicted here may serve as a definite reference when attempting to simulate the ghost sector of the theory.

From the point of view of the SDEs, one may envisage various improvements. To begin with, the replacement of the fully-dressed ghost-gluon vertex by the tree-level expression inside the ghost SDE ought to be ameliorated. This, in turn, would require the treatment of the corresponding vertex SDE, for a general ξ, in the spirit of the analysis presented in the Landau gauge [43]. To be sure, subtractive instead of multiplicative renormalizability is another longstanding drawback in practically all types of SDE analysis; however, given that this problem cannot be even solved within the context of the (easier) Landau gauge, the prospects for a notable refinement in this particular direction seem rather reduced.

It is also clear that additional theoretical work at the level of the gluon propagator is an absolute requirement before any firm statements could be made. In particular, no study related to the possibility of gluon mass generation away from the Landau gauge has been carried out to date; in the present work we have simply assumed the realization of this scenario, based almost exclusively on the limited lattice evidence of [34]. In particular, it would be essential to derive the dynamical equation that governs the evolution of the gluon mass for an arbitrary ξ, and explore the type of solutions it might admit. This task is technically rather complex, mainly due to the proliferation of terms with respect to the Landau gauge case. Calculations in this direction are already in progress, and we hope to report progress in the near future.

Acknowledgments

The research of J. P. is supported by the Spanish MEYC under grant FPA2011-23596 and the Generalitat Valenciana under grant PrometeoII/2014/066. The work of A. C. A is supported by the National Council for Scientific and Technological Development - CNPq under the grant 306537/2012-5 and project 473260/2012-3, and by São Paulo Research Foundation - FAPESP through the project 2012/15643-1.

Appendix A: Derivation of the Nielsen identities

The action $\Gamma^{(0)}$ of the SU(N) Yang-Mills theory can be written as the sum of three terms,

$$\Gamma^{(0)} = S_{\rm YM} + S_{\rm GF+FPG} + S_{\rm BV}, \tag{A1}$$

where the first term corresponds to the classical action

$$S_{\rm YM} = -\frac{1}{4}\int \mathrm{d}^4x\, F^a_{\mu\nu}F^{\mu\nu}_a; \qquad\qquad F^a_{\mu\nu} = \partial_\mu A^a_\nu - \partial_\mu A^a_\nu + g f^{abc} A^b_\mu A^c_\nu, \tag{A2}$$

while the second to the gauge fixing and its associated Faddeev-Popov action, written as

$$S_{\rm GF+FPG} = s\int \mathrm{d}^4x\, \bar{c}^a \left(\mathcal{F}^a - \frac{\xi}{2}b^a\right). \tag{A3}$$

In the equation above b^a is the Nakanishy-Lautrup multiplier, $\bar{c}^a$ the antighost field, while $\mathcal{F}^a$ represents, for the moment, an arbitrary gauge fixing function. The only restriction on this latter function is that it allows for the inversion of the tree-level two-point functions of the A–b sector, thus yielding the field propagators (in what follows we will use an off-shell formalism, keeping explicitly the b fields, which, otherwise, can be eliminated by making use of their trivial equation of motion). Finally, s is the BRST symmetry operator that acts on the elementary fields according to

$$sA^a_\mu = \underbrace{\left(\partial_\mu\delta^{ab} + g f^{acb}A^c_\mu\right)}_{\mathcal{D}^{ab}_\mu} c^b; \qquad sc^a = -\frac{1}{2}g f^{abc}c^b c^c; \qquad s\bar{c}^a = b^a; \qquad sb^a = 0, \tag{A4}$$

with $\mathcal{D}^{ab}_\mu$ the usual covariant derivative.

As can be explicitly seen above, the BRST variations of the gauge and ghost fields are non-linear in the quantum fields; their renormalization is ensured by the introduction of external sources, known as antifields, in the third term of (A1), reading

$$S_{\rm BV} = \int \mathrm{d}^4x\, \left(A^{*a}_\mu sA^\mu_a + c^*_a sc^a\right). \tag{A5}$$

The tree-level action (A1) will then satisfy the Slavnov-Taylor (ST) identity

$$\mathcal{S}(\Gamma^{(0)}) = 0; \qquad \mathcal{S}(\Gamma^{(0)}) = \int \mathrm{d}^4x \left(\frac{\delta\Gamma^{(0)}}{\delta A^{*a}_\mu} \frac{\delta\Gamma^{(0)}}{\delta A^\mu_a} + \frac{\delta\Gamma^{(0)}}{\delta c^*_a} \frac{\delta\Gamma^{(0)}}{\delta c^a} + b^a \frac{\delta\Gamma^{(0)}}{\delta \bar{c}^a} \right). \tag{A6}$$

As the theory is anomaly-free, the ST identity (A6) holds also for the full vertex functional Γ.

If we extend the BRST to include also the gauge parameter ξ, we obtain an extended ST identity that gives control over the gfp-dependence of the Green's function of the theory [36, 37]. Writing[7]

$$s\xi = \chi; \qquad s\chi = 0, \tag{A7}$$

one obtains that

$$S_{\mathrm{GF+FPG}} = \int \mathrm{d}^4x \left(b^a \mathcal{F}^a - \frac{\xi}{2} b_a^2 - \bar{c}^a s\mathcal{F}^a \right) + \int \mathrm{d}^4x\, \bar{c}^a \left(\frac{1}{2}\chi b^a - \chi \frac{\partial \mathcal{F}^a}{\partial \xi} \right), \tag{A8}$$

and therefore the tree-level action satisfies the extended ST identity

$$\mathcal{S}'(\Gamma^{(0)}) = 0; \qquad \mathcal{S}'(\Gamma^{(0)}) = \mathcal{S}(\Gamma^{(0)}) + \chi \frac{\partial \Gamma^{(0)}}{\partial \xi}. \tag{A9}$$

Again, the identity above is valid for the full vertex functional Γ; taking then a derivative with respect to χ and setting it to zero afterwards, one obtains the NI

$$\left.\frac{\partial\Gamma}{\partial\xi}\right|_{\chi=0} = \int \mathrm{d}^4x \left(\frac{\delta\Gamma}{\delta A^{*a}_\mu} \frac{\delta^2\Gamma}{\partial\chi \delta A^\mu_a} - \frac{\delta^2\Gamma}{\partial\chi \delta A^{*a}_\mu} \frac{\delta\Gamma}{\delta A^\mu_a} - \frac{\delta^2\Gamma}{\partial\chi \delta c^*_a} \frac{\delta\Gamma}{\delta c^a} - \frac{\delta\Gamma}{\delta c^*_a} \frac{\delta^2\Gamma}{\partial\chi \delta c^a} - b^a \frac{\delta^2\Gamma}{\partial\chi \delta \bar{c}^a} \right)\Bigg|_{\chi=0}. \tag{A10}$$

1. Linear covariant gauges

Even though the NI (A10) holds irrespectively of the gauge fixing functional chosen, we will specialize from now on to the case of linear covariant (or R_ξ) gauges, which are identified by the choice of the following gauge fixing function

$$\mathcal{F}^a = \partial^\mu A^a_\mu, \tag{A11}$$

and, in our conventions, the non negativity condition on ξ [32], needed to ensure that the (Euclidean) path integral over the b fields is Gaussian.

[7] A pair of variables (u, v) such that $su = v$ and $sv = 0$ is called a BRST doublet; notice that also $\bar{c}$ and b form such a doublet.

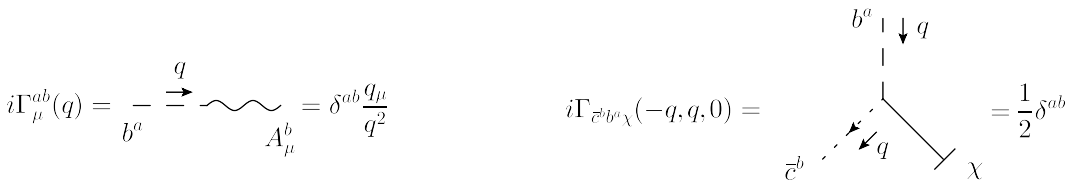

FIG. 10: Feynman rules for the b-sector. Notice that, due to the b equation (A14), there are no possible quantum correction to these Feynman rules.

Thus in the two-point gluon sector the R_ξ gauge fixing yields the tree-level propagators AA, Ab, bb given respectively by

$$i\Delta^{ab}_{\mu\nu}(q) = -i\delta^{ab}\frac{1}{q^2}\left[P_{\mu\nu}(q) + \xi\frac{q_\mu q_\nu}{q^2}\right]; \qquad i\Delta^{ab}_{\mu}(q) = \delta^{ab}\frac{q_\mu}{q^2}; \qquad i\Delta^{ab} = 0. \tag{A12}$$

For the ghost sector the tree-level propagator is instead written as

$$iD^{ab}(q) = i\delta^{ab}\frac{1}{q^2}. \tag{A13}$$

Now observe that the b-equation

$$\frac{\delta\Gamma}{\delta b^a} = \partial^\mu A^a_\mu - \xi b^a + \frac{1}{2}\bar{c}^a\chi, \tag{A14}$$

implies that the b dependence is confined at tree-level, and so will the mixed bA propagator Δ_μ (and any vertex involving the b field for that matter). Thus, beyond tree-level the only non-trivial propagators will be

$$i\Delta^{ab}_{\mu\nu}(q) = -i\delta^{ab}\left[P_{\mu\nu}(q)\Delta(q^2) + \xi\frac{q_\mu q_\nu}{q^2}\right]; \qquad iD^{ab}(q) = i\delta^{ab}\frac{F(q^2)}{q^2}, \tag{A15}$$

where $F(q^2)$ is the ghost dressing function. The Feynman rules for vertices involving fields and/or antifields can be found in [44]; they need to be supplemented with one more rule, describing the coupling of the χ source to a b and a $\bar{c}$ fields, which can be read off directly from Eq. (A14):

$$i\Gamma_{\bar{c}^b b^a \chi}(-q,q,0) = \frac{1}{2}\delta^{ab}. \tag{A16}$$

As already mentioned, this vertex will not receive quantum corrections, and will be completely fixed by its tree-level value given above. The Feynman rules involving the Nakanishy-Lautrup multiplier b are summarized in Fig. 10.

In addition, the Faddeev-Popov equation

$$\frac{\delta\Gamma}{\delta\bar{c}^a} + \partial^\mu\frac{\delta\Gamma}{\delta A^{*a}_\mu} = \frac{1}{2}\chi b^a, \tag{A17}$$

implies that beyond tree-level the dependence on $\bar{c}$ of the vertex functional Γ can only be realized through the combination $\widetilde{A}^{*a}_{\mu} = A^{*a}_{\mu} + \partial_{\mu} c^a$; indeed, if $\Gamma = \Gamma[\widetilde{A}^*]$ one has

$$\frac{\delta\Gamma}{\delta\bar{c}^a(x)} = \int \mathrm{d}^4 y \, \frac{\delta\Gamma}{\delta\widetilde{A}^b_{\mu}(y)} \frac{\delta\widetilde{A}^b_{\mu}(y)}{\delta\bar{c}^a(x)} = \int \mathrm{d}^4 y \, \frac{\delta\Gamma}{\delta\widetilde{A}^b_{\mu}(y)} \partial^y_{\mu}\delta(x-y) = -\partial^x_{\mu} \frac{\delta\Gamma}{\delta\widetilde{A}^b_{\mu}(x)} = -\partial^x_{\mu} \frac{\delta\Gamma}{\delta A^b_{\mu}(x)}, \tag{A18}$$

with the last step due to the linearity of the field transformation employed. Making then the change of variable $A^*_{\mu} \to \widetilde{A}^*_{\mu}$, and introducing the reduced functional $\widetilde{\Gamma}$ through

$$\widetilde{\Gamma} = \Gamma - \int \mathrm{d}^4 x \, \left[b^a \partial^{\mu} A^a_{\mu} - \frac{\xi}{2} (b^a)^2 \right], \tag{A19}$$

one can restrict the sum over fields appearing in the rhs of Eq. (A10) to the pairs $(A^a_{\mu}, \widetilde{A}^{*a}_{\mu})$ and (c^a, c^*_a) alone. In the NI analysis carried out in this work we have use only 'tilded' quantities, and therefore suppressed this symbol everywhere. Incidentally, notice that it is Eq. (A19) that implies the tree-level result $\Gamma^{(0)}_{A^a_{\mu} A^b_{\nu}}(q) = iq^2 \delta^{ab} P_{\mu\nu}(q)$.

The final form of the NI used is then written as

$$\left.\frac{\partial\Gamma}{\partial\xi}\right|_{\chi=0} = \int \mathrm{d}^4 x \, \left(\frac{\delta\Gamma}{\delta A^{*a}_{\mu}} \frac{\delta^2\Gamma}{\partial\chi \delta A^{\mu}_a} - \frac{\delta^2\Gamma}{\partial\chi \delta A^{*a}_{\mu}} \frac{\delta\Gamma}{\delta A^{\mu}_a} - \frac{\delta^2\Gamma}{\partial\chi \delta c^*_a} \frac{\delta\Gamma}{\delta c^a} - \frac{\delta\Gamma}{\delta c^*_a} \frac{\delta\Gamma}{\partial\chi \delta c^a} \right) \Bigg|_{\chi=0}. \tag{A20}$$

Using the technique developed in [52], one can write the complete solution to the NI above [53]. Rewriting Eq. (A20) as[8]

$$\left.\frac{\partial\Gamma}{\partial\xi}\right|_{\chi=0} = \int \mathrm{d}^4 x \, \left(\frac{\delta\Psi}{\delta A^{*a}_{\mu}} \frac{\delta\Gamma}{\delta A^{\mu}_a} - \frac{\delta\Psi}{\delta A^a_{\mu}} \frac{\delta\Gamma}{\delta A^{*\mu}_a} + \frac{\delta\Psi}{\delta c^a} \frac{\delta\Gamma}{\delta c^*_a} - \frac{\delta\Psi}{\delta c^*_a} \frac{\delta\Gamma}{\delta c^a} \right) \Bigg|_{\chi=0}; \quad \Psi \equiv \frac{\partial\Gamma}{\partial\chi}, \tag{A21}$$

its full solution is given by [53]

$$\Gamma = \sum_{n\geq 0} \frac{1}{n!} \xi^n \Gamma_n; \qquad \Gamma_n = \left[\Delta^n_{\Psi} \Gamma_0 \right] \big|_{\xi=0}, \tag{A22}$$

where $\Gamma_0 = \Gamma|_{\xi=0}$ is the vertex functional in the Landau gauge, and in the R_{ξ} gauges the Lie operator Δ_{Ψ} reads

$$\Delta_{\Psi} X = \int \mathrm{d}^4 x \, \left(\frac{\delta X}{\delta A^a_{\mu}} \frac{\delta\Psi}{\delta A^{*\mu}_a} + \frac{\delta X}{\delta A^{*a}_{\mu}} \frac{\delta\Psi}{\delta A^{\mu}_a} + \frac{\delta X}{\delta c^*_a} \frac{\delta\Psi}{\delta c^a} + \frac{\delta X}{\delta c^a} \frac{\delta\Psi}{\delta c^*_a} \right) + \frac{\partial X}{\partial\xi}. \tag{A23}$$

[8] The sign differences with respect to [53] are due to the different conventions used. In particular, our Yang-Mills action is obtained from the one of [53] through the replacements: $\bar{c} \to -\bar{c}$, $b \to -b$, $c^* \to -c^*$ and $\alpha \to -\xi$ (which also implies $\theta \to -\chi$ when introducing the doublet partner of the gfp parameter).

If $\xi \ll 1$ one can linearize Eq. (A22); the coefficient of the linear term Γ_1 is then obtained by applying the Lie operator on the Landau vertex functional Γ_0. As the latter does not depend on the gfp ξ, within the linear approximation one has

$$\partial_\xi \Gamma = \Gamma_1, \tag{A24}$$

with

$$\begin{aligned}\Gamma_1 &= \int \mathrm{d}^4x \left(\frac{\delta\Gamma_0}{\delta A^a_\mu}\frac{\delta\Psi}{\delta A^{*\mu}_a} + \frac{\delta\Gamma_0}{\delta A^{*a}_\mu}\frac{\delta\Psi}{\delta A^\mu_a} + \frac{\delta\Gamma_0}{\delta c^*_a}\frac{\delta\Psi}{\delta c^a} + \frac{\delta\Gamma_0}{\delta c^a}\frac{\delta\Psi}{\delta c^*_a}\right)\Big|_{\xi=0} \\ &= \int \mathrm{d}^4x \left(\frac{\delta\Gamma_0}{\delta A^{*a}_\mu}\frac{\delta^2\Gamma_0}{\partial\chi\delta A^\mu_a} - \frac{\delta^2\Gamma_0}{\partial\chi\delta A^{*a}_\mu}\frac{\delta\Gamma_0}{\delta A^\mu_a} - \frac{\delta^2\Gamma_0}{\partial\chi\delta c^*_a}\frac{\delta\Gamma_0}{\delta c^a} - \frac{\delta\Gamma_0}{\delta c^*_a}\frac{\delta\Gamma_0}{\partial\chi\delta c^a}\right). \end{aligned} \tag{A25}$$

We then see that the approximation employed in this work on the full NIs are equivalent to differentiating Eq. (A24) with respect to a ghost and an antighost [Eq. (3.8)], or two gluon fields [Eq. (3.16)].

[1] A. Cucchieri and T. Mendes, PoS **LAT2007**, 297 (2007), 0710.0412.

[2] A. Cucchieri and T. Mendes, PoS **QCD-TNT09**, 026 (2009), 1001.2584.

[3] I. L. Bogolubsky, E. M. Ilgenfritz, M. Muller-Preussker, and A. Sternbeck (2007), arXiv:0710.1968 [hep-lat].

[4] I. Bogolubsky, E. Ilgenfritz, M. Muller-Preussker, and A. Sternbeck, Phys. Lett. **B676**, 69 (2009), 0901.0736.

[5] O. Oliveira and P. Silva, PoS **LAT2009**, 226 (2009), 0910.2897.

[6] J. M. Cornwall, Phys. Rev. **D26**, 1453 (1982).

[7] C. W. Bernard, Nucl. Phys. **B219**, 341 (1983).

[8] J. F. Donoghue, Phys. Rev. **D29**, 2559 (1984).

[9] O. Philipsen, Nucl. Phys. **B628**, 167 (2002), hep-lat/0112047.

[10] A. C. Aguilar and A. A. Natale, JHEP **08**, 057 (2004), hep-ph/0408254.

[11] A. C. Aguilar, D. Binosi, and J. Papavassiliou, Phys. Rev. **D84**, 085026 (2011), 1107.3968.

[12] D. Binosi, D. Ibañez, and J. Papavassiliou, Phys. Rev. **D86**, 085033 (2012), 1208.1451.

[13] A. C. Aguilar, D. Binosi, and J. Papavassiliou, Phys. Rev. **D89**, 085032 (2014), 1401.3631.

[14] P. Boucaud et al., JHEP **06**, 099 (2008), 0803.2161.

[15] A. C. Aguilar, D. Binosi, and J. Papavassiliou, Phys. Rev. **D78**, 025010 (2008), 0802.1870.

[16] D. Dudal, J. A. Gracey, S. P. Sorella, N. Vandersickel, and H. Verschelde, Phys. Rev. **D78**, 065047 (2008), 0806.4348.

[17] C. S. Fischer, A. Maas, and J. M. Pawlowski, Annals Phys. **324**, 2408 (2009), 0810.1987.

[18] M. Pennington and D. Wilson, Phys. Rev. **D84**, 119901 (2011), 1109.2117.

[19] D. R. Campagnari and H. Reinhardt, Phys. Rev. **D82**, 105021 (2010), 1009.4599.

[20] A. Sternbeck, L. von Smekal, D. Leinweber, and A. Williams, PoS **LAT2007**, 340 (2007), 0710.1982.

[21] P. O. Bowman et al., Phys. Rev. **D76**, 094505 (2007), hep-lat/0703022.

[22] A. Ayala, A. Bashir, D. Binosi, M. Cristoforetti, and J. Rodriguez-Quintero, Phys. Rev. **D86**, 074512 (2012), 1208.0795.

[23] A. C. Aguilar, D. Binosi, and J. Papavassiliou, Phys. Rev. **D86**, 014032 (2012), 1204.3868.

[24] A. C. Aguilar, D. Binosi, and J. Papavassiliou, Phys. Rev. **D88**, 074010 (2013), 1304.5936.

[25] P. Maris and P. C. Tandy, Phys. Rev. **C60**, 055214 (1999), nucl-th/9905056.

[26] A. C. Aguilar, D. Binosi, J. Papavassiliou, and J. Rodriguez-Quintero, Phys. Rev. **D80**, 085018 (2009), 0906.2633.

[27] A. C. Aguilar, D. Binosi, and J. Papavassiliou, JHEP **1007**, 002 (2010), 1004.1105.

[28] S.-x. Qin, L. Chang, Y.-x. Liu, C. D. Roberts, and D. J. Wilson, Phys. Rev. **C84**, 042202 (2011), 1108.0603.

[29] L. Chang and C. D. Roberts, Phys. Rev. Lett. **103**, 081601 (2009), 0903.5461.

[30] I. C. Cloet and C. D. Roberts, Prog. Part. Nucl. Phys. **77**, 1 (2014), 1310.2651.

[31] D. Binosi, L. Chang, J. Papavassiliou, and C. D. Roberts (2014), 1412.4782.

[32] K. Fujikawa, B. W. Lee, and A. I. Sanda, Phys. Rev. **D6**, 2923 (1972).

[33] A. Cucchieri, T. Mendes, and E. M. Santos, Phys. Rev. Lett. **103**, 141602 (2009), 0907.4138.

[34] A. Cucchieri, T. Mendes, G. M. Nakamura, and E. M. Santos, PoS **FACESQCD**, 026 (2010), 1102.5233.

[35] C. D. Roberts and A. G. Williams, Prog. Part. Nucl. Phys. **33**, 477 (1994), hep-ph/9403224.

[36] N. K. Nielsen, Nucl. Phys. **B101**, 173 (1975).

[37] N. K. Nielsen, Nucl. Phys. **B97**, 527 (1975).

[38] L. Landau and I. Khalatnikov, Sov. Phys. JETP **2**, 69 (1956).

[39] E. Fradkin, Zh. Eksp. Teor. Fiz. **29**, 258 (1955).

[40] D. C. Curtis and M. R. Pennington, Phys. Rev. **D42**, 4165 (1990).

[41] A. Kizilersu and M. Pennington, Phys. Rev. **D79**, 125020 (2009), 0904.3483.

[42] A. C. Aguilar, D. Binosi, D. Ibañez, and J. Papavassiliou, Phys. Rev. **D89**, 085008 (2014), 1312.1212.

[43] A. C. Aguilar, D. Ibañez, and J. Papavassiliou, Phys. Rev. **D87**, 114020 (2013), 1303.3609.

[44] D. Binosi and J. Papavassiliou, JHEP **0811**, 063 (2008), 0805.3994.

[45] M. Tissier and N. Wschebor, Phys. Rev. **D84**, 045018 (2011), 1105.2475.

[46] D. Binosi and J. Papavassiliou, Phys. Rept. **479**, 1 (2009), 0909.2536.

[47] A. P. Szczepaniak and E. S. Swanson, Phys. Rev. **D65**, 025012 (2002), hep-ph/0107078.

[48] A. P. Szczepaniak, Phys. Rev. **D69**, 074031 (2004), hep-ph/0306030.

[49] D. Epple, H. Reinhardt, W. Schleifenbaum, and A. Szczepaniak, Phys. Rev. **D77**, 085007 (2008), 0712.3694.

[50] A. P. Szczepaniak and H. H. Matevosyan, Phys. Rev. **D81**, 094007 (2010), 1003.1901.

[51] A. Bashir and A. Raya, Phys. Rev. **D66**, 105005 (2002), hep-ph/0206277.

[52] D. Binosi and A. Quadri, Phys. Rev. **D85**, 121702 (2012), 1203.6637.

[53] A. Quadri (2014), 1412.6772.